Reliability-based design for debris flow barriers

Reliability-based design for debris flow barriers

Vagnon, Federico

Department of Earth Science, University of Turin, Via Valperga Caluso 35, 10125, Turin, Italy

Corresponding author: federico.vagnon@unito.it, Tel: +39 0116705325

Ferrero, Anna Maria

Department of Earth Science, University of Turin, Via Valperga Caluso 35, 10125, Turin, Italy

anna.ferrero@unito.it

Alejano, Leandro R.

Department of Natural Resources and Environmental Engineering, University of Vigo, Galicia, Spain

alejano@uvigo.es

Abstract

In the European Union since 2010, the design of any type of structures must comply with EN-1997 Geotechnical Design (CEN 2004) (EC7) referring to engineering projects in the rock mechanics field. However, the design of debris flow countermeasures in compliance with EC7 requirements is not feasible: EC7 uses partial safety factors for design calculations, but safety factors are not provided for phenomena such as debris flows and rock falls. Consequently, how EC7 can be applied to the design of debris flow barriers is not clear, although the basic philosophy of reliability-based design (RBD), as defined in EN1990 (CEN 2002) and applicable to geotechnical applications, may be a suitable approach.

However, there is insufficient understanding of interactions between debris flows and structures to support RBD application to debris flow barrier design, as full-scale experimental data are very limited and difficult to obtain. Laboratory data are available but they are governed by scale effects that limit their usefulness for full-scale problems.

The article describes an analysis, using the first-order reliability method (FORM), of two different datasets, one obtained through laboratory experiments and the other reflecting historical debris flow events in the Jiangjia Ravine (China). Statistical analysis of laboratory data enabled a definition of the statistical distributions of the parameters that primarily influence debris flow and barrier interactions. These statistical distributions were then compared to the field data to explore the links between flume experiments and full-scale problems.

This paper reports a first attempt to apply RBD to debris flow countermeasures, showing how the choice of the target probability of failure influences the barrier design resistance value. An analysis of the factors governing debris flows highlights the applicability and limitations of EN1990 and EN1997 in the design of these rock engineering structures.

Keywords

Eurocode 7 (EC7); Reliability index; First-order reliability method (FORM); Partial safety factor; Debris flow; Mitigation design.

1. Introduction

Debris flows are extremely rapid gravitational movements that occur widely on Earth. They are among the most devastating landslide processes owing to their unpredictability, their total absence of premonitory signals, their high velocities and their long travel distances. Many mitigation strategies have been developed in recent years to reduce the associated risk, and both active and passive measures are used to reduce the magnitude and frequency of debris flows and to change the vulnerability of debris flow basins. Although passive measures (hazard mapping and correct land-use planning) are more advisable than active measures (protection structures), the latter are often essential in order to reduce risk (Jakob and Hungr 2005).

Common active measures can be classified as rigid measures – such as close-type check dams, open-type sabo dams and concrete-slit sabo dams – and flexible measures, mainly net barriers designed as a function of the deformation capability. Although very different in terms of components, drainage capacity and construction methodology, their main requirement is to counteract the impact forces underlying debris flow, dissipate its kinetic energy and totally or partially retain the flowing material.

The design of countermeasures is still an open issue. While there are many approaches to evaluating impact pressure (Hungr et al. 1984; Armanini and Scotton 1992; Hubl et al. 2009; Vagnon and Segalini 2016), uncertainty regarding flow characteristics (velocity and thickness) tends to be high and difficult to quantify (Jakob and Hungr 2005; Vagnon et al. 2015).

With this issue in mind, the Geotechnical Engineering Office of the Government of Hong Kong introduced the first technical basis for the design of standardized debris-resisting barrier modules to mitigate natural terrain landslide hazards (Sun et al. 2003). While its report analyses different debris flow run-out models and barrier types, there is no mention of the probability of failure of these structures. In 2009, the Austrian Standard Institute proposed the Österreichischen

66 Normungsinstituts Regeln (ONR) 24800 series to design torrent control structures. ONR 24802
67 (2011) defines loading scenarios for debris flow protection structures, specifically providing
68 information on limit state design and failure mode for check dams, as well as partial safety factors
69 for structural (STR) and geotechnical (GEO) limit state actions.

70 When considering the design of debris flow barriers, uncertainties regarding all debris flow phases
71 are difficult to quantify; consequently, since the degree of reliability is not evaluated, the probability
72 of failure remains unknown.

73 The interaction between debris flow and barrier is only dealt with in passing in EN-1997
74 Geotechnical Design (CEN 2004) (EC7), and although protection structures are widely used for
75 mitigation purposes, there are no specific indications regarding their design. In previous works
76 (Vagnon et al. 2016; Vagnon et al. 2017), the authors highlighted limitations in the applicability of
77 EC7, and in particular the limit state design (LSD) approach to designing this type of structure due
78 to the limited availability of experimental data. The set of proposed partial factors are clearly
79 inadequate since they refer only to flow density and internal friction angle and neglect other
80 relevant debris flow parameters such as flow velocity and thickness.

81 Uncertainties are considered in EC7: the concept of characteristic value introduced by the LSD
82 approach allows a cautiously mean value to be selected, averaged over the failure surface and taking
83 into account variability and uncertainties in the very definition of the parameter. However, spatial
84 correlations between the same kind of parameters and cross-correlations between different
85 parameters are still missing (Low and Phoon 2015). Many studies have demonstrated the presence
86 of cross-correlations that are not entirely negligible, especially between soil parameters. Concerning
87 debris flow, in a recent work, Vagnon and Segalini (2016) demonstrated a correlation between
88 velocity and flow height.

89 For all the above reasons, the authors believe that a design approach based on a target reliability

90 index (Duncan 2000; Baecher and Christian 2003) could be a useful complementary tool in defining
91 a uniform probability of failure for geotechnical structures. Reliability-based design (RBD) can
92 provide additional insights into EC7 design and can be applied where partial factors have yet to be
93 proposed (by EC7) to cover the uncertainties associated with less common parameters (Low and
94 Phoon 2015), as is the case of debris flow countermeasures. Moreover, as stated by Duncan (2000),
95 reliability calculations are a means for evaluating the combined effects of uncertainties and for
96 distinguishing between conditions where uncertainties are very high, a clear example of which is
97 evaluation of debris flow impact pressure.

98 RBD is widely used, especially in civil engineering, and has been applied to the study of slope
99 stability (Li et al. 2016; Zhao et al. 2016; McGuire and VandenBerge 2017; Huang et al. 2018).
100 EN 1990 (2002), the European standard that describes the basis for structural design, requires
101 structures to be designed with an appropriate degree of reliability, which varies as a function of
102 three reliability classes (RCs) for the ultimate limit state. The problem, however, is that there is no
103 clear indication of the best class to choose and EC7, moreover, does not suggest any relationship
104 between the RCs and geotechnical classes (Section 2.1 EC7). Normally, a reliability index greater
105 than 3.8 for a 50-year reference period (corresponding to RC2) is recommended.

106 The purpose of this paper is to perform RBD for debris flow protection barriers and to propose a
107 methodology for evaluating the probability of failure for such complex problems. Two databases,
108 one obtained from laboratory experimental tests and one based on real events in the Jiangjia Ravine
109 basin in China, are used as a basis for an analysis of the complementary relationship between EC7
110 and RBD.

111 This paper, which, as far as we are aware, represents a first attempt to apply RBD to debris flow
112 protection barriers, shows how the choice of a target probability of failure influences the resistance
113 value of the barrier design. The analysis covers factors governing debris flow as well as variations –

as a function of the probability of failure – in partial safety factors computed using the Excel spreadsheet platform for the first-order reliability method (FORM) developed by Low and Tang (2007).

2. FORM procedures

Reliability analyses are commonly expressed by the Hasofer-Lind (1974) reliability index β, which can be related to probability of failure, P_f. P_f can be estimated as follows:

$$P_f \approx 1 - \Phi(\beta) = \Phi(-\beta) \quad (1)$$

where Φ is the normal cumulative probability function.

Since the reliability index is calculated by minimizing the quadratic form tangent to the limit state surface at the most probable failure point (Figure 1), defining β makes it possible to determine the coordinates of what is called the design point (x*). Physically denoted is the tangency of the expanding dispersion ellipsoid with the failure domain surface.

Figure 1. Illustration of the reliability index in a plane with two negatively correlated random variables.

While numerous methods to perform reliability analyses have been described, e.g., by Ditlevsen (1981), Ang and Tang (1984), Madsen et al. (1986), Low and Tang (1997), Haldar and Mahadevan (1999), Melchers (1999) and Baecher and Christian (2003), the most consistent approach is FORM, which is a useful spreadsheet-automated constrained optimization approach (Low and Tang, 2007).

In the spreadsheet, the equation for evaluating β is:

$$\beta = \min_{x \in f} \sqrt{\vec{n}^{T}[R]^{-1}\vec{n}} \quad (2)$$

where $\vec{n}$ is a dimensionless vector defined as $\vec{n} = (x-\mu^{N})/\sigma^{N}$, x is a vector representing the set of random variables, μ^{N} and σ^{N} are the vectors of normal mean and normal standard deviation evaluated using Rackwitz–Fiessler equations (1978), R is the correlation matrix, and f is the failure domain.

For each value of n_i trialled by the Excel Solver, a short and simple Excel VBA code automates the computation of x_i from n_i, for use in the constraint performance function g(x) = 0, via $x_i=F^{-1}\Phi[(n_i)]$, where Φ is the standard normal distribution and F is the original non-normal distribution.

The use of Equation 2 is necessary because, as will be discussed in later sections, the leading variables in debris flow phenomena follow non-normal distributions.

3. RBD versus EC7 design

EC7 is based on LSD, a semi-probabilistic method in which partial factors are applied to characteristic parameter values in order to account for parameter uncertainty and so achieve designs with a certain target reliability (Figure 2).

Figure 2. EC7 limit state design: probabilities of actions and material resistance.

The aim underlying LSD, which is based on reliability analyses, is to provide structures with a uniform probability of failure (Figure 2). The fundamental principle is to verify that design

160 resistance is always greater than the effect of action. This verification can be done by following one
161 of three different design approaches, described in detail in Section 2.4.7.3.4 of EC7 (EN 1997-
162 1:2004). Broadly speaking, EC7 requires the use of partial safety factors aimed at reducing
163 resistance and enhancing actions. While the efficacy of this approach has been demonstrated in civil
164 engineering, its efficacy in the geotechnical field has raised many doubts, particularly in rock
165 mechanics, where variability and uncertainty associated with materials (soil and rock) play a
166 fundamental role (Harrison 2014; Lamas et al. 2014; Vagnon et al. 2020). Furthermore, in EC7 a
167 number of geotechnical problems are not adequately covered, including debris flows and rock falls.
168 The partial safety factor approach does not provide any information on the probability of failure of
169 the designed structures and has never been investigated for debris flow protection purposes.

170 The above considerations are pertinent to understanding why an RBD analysis is required for
171 certain complex geotechnical applications, including the design of debris flow protection structures.
172 Some authors (Callisto 2010; Low and Phoon 2015) have highlighted how applying the same partial
173 safety factors in problems with different levels of uncertainty may not result in the same target
174 failure probability. By fixing the reliability index, however, the probability of failure remains the
175 same, i.e., it is not dependent on the problem type and or the level of parametric uncertainty. Partial
176 safety factors can be back-calculated from the RBD by fixing characteristic values for the random
177 variables and by assessing the design point coordinates.

178 The dearth of data to perform statistical analyses may be considered the main limitation of an RBD
179 approach. This is especially true in the case of debris flow, for which databases for the main
180 parameters involved (velocity, v_f, thickness, h_f, and the dynamic coefficient, α) are difficult to
181 obtain.

182 In sum, in the case of debris flow phenomena, RBD provides insights missing from EC7 design
183 when statistical information on key parameters is available, when partial factors have not been

184 proposed and when input parameters are correlated.

185

186 **4. Statistical analysis of laboratory and real debris flow motion characteristics**

187 As stated above, the main limitation of the RBD approach is the availability of data to conduct
188 robust statistical analyses and to define the probability distribution of the parameters considered in
189 the performance function. Evaluated below is the fit between probabilistic models and debris flow
190 motion data, using a dataset of experimental laboratory tests performed by the authors (laboratory
191 dataset) and a dataset of 139 real events that occurred in the Jiangjia Ravine basin in China (field
192 dataset).

193 The laboratory dataset contains flow velocity and thickness values as well as the dynamic
194 coefficients for 82 experimental laboratory flume tests (Figure 3) in which a debris flow was
195 created by the rapid emptying of a hopper into the flume. Different material volumes (0.065 to
196 0.075 m^3) and different flume slopes (30° to 35°) were used in the experiments. Velocity, flow
197 height and the impact force were recorded using four ultrasonic levels located along the centre line
198 of the channel and four load cells installed directly on the barrier.

199 The dynamic coefficient is a dimensionless parameter used in hydrodynamic models to evaluate
200 impact pressure on obstacles/structures. Dependent on the grain size distribution of the flow and
201 barrier/obstacle characteristics (Vagnon and Segalini 2016), for the purposes of this research it was
202 indirectly derived from experimental and field data using Hungr et al.'s hydrodynamic model
203 (1984):

204

205 $$\alpha = \frac{p_{measured}}{\rho v_f^2} \quad (3)$$

206

where $p_{measured}$ is the impact pressure measured in Pa, ρ is the flow density in kg/m^3, and v_f is the impacting flow velocity in m/s.

A more detailed description of laboratory apparatus and instruments can be found in Vagnon and Segalini (2016).

Figure 3. Flume setup and location of measurement devices.

The field dataset includes thickness (h_f), density (ρ), channel width (B), duration (t) and velocity (v_f) values for 139 historical events that took place between 1961 and 2000 in the Jiangjia Ravine basin located in the Dongchuan area of Yunnan Province in China (Zhang and Xiong 1997; Kang et al. 2006, 2007; Hong et al. 2015). This basin experiences numerous debris flow events each year (up to 28) that cause great damage to local infrastructure (Hong et al. 2015). Debris flows, which mainly occur during the rainy season (June to September), lead to highly fractured rocks and colluvium being eroded and rapidly carried to the valley floor (Zhou and NG 2010).

An unparalleled record is available of long-term observations of this site by the Dongchuan Debris Flow Observation and Research Station (DDFORS), which set up a permanent monitoring station in the downstream area in the 1960s. Flow velocity is measured by a stopwatch in two marked sections along the gully, front head thickness is measured by a supersonic lever meter and surge density is measured by direct sampling of debris flows. The dynamic coefficient was back-calculated using Equation 3. Table 1 shows the main features of the datasets.

Table 1. Principal laboratory and field dataset features.

The raw data from the two datasets was used to perform a statistical analysis for the parameters listed in Table 2.

Table 2. Main statistical parameters for the laboratory and field datasets.

Each distribution was sorted into k-intervals in order to obtain the relative frequency of the real data. The following equation was used to evaluate the number of classes:

$$k = 2n^{0.4} \quad (4)$$

where k is the number of classes and n is the dimension of the population data. For the laboratory and field datasets, the number of classes was, respectively, 12 and 14.

The basic idea behind this statistical analysis, in addition to defining probabilistic models for each parameter, was to evaluate the interchangeability of models between laboratory and field datasets. The probabilistic analysis was performed first for the laboratory measurements and then for the field measurements.

The statistical distribution of laboratory measurements for v_f, h_f and α were simulated using seven probabilistic models: normal, lognormal, exponential, Gumbel, generalized extreme value (GEV), Gamma and Weibull. Since there was no prior knowledge on debris flow phenomena, the suitability of each model for predicting distributions of v_f, h_f and α was not known. While the Gumbel and GEV distribution have been used in hydraulic analyses to evaluate the return period for a specific river flood height, there are no suggestions of their applicability to the debris flow field.

The goal was to verify which probability distributions best fitted the laboratory data and then try to

253 apply those distributions to the field data. The fit of each probabilistic model was assessed using
254 two statistical goodness-of-fit (GoF) tests: Chi-square (χ^2) and Anderson–Darling (AD). The
255 probabilistic model not rejected by both GoF tests was then used as input for the Low and Tang
256 (2004) spreadsheet.

257 Table 3 lists the results of the GoF tests for the three considered variables, v_f, h_f and α. The results
258 of GoF tests highlighted that: (i) the GEV model is suitable for simulating all three parameters, and
259 (ii) the Gumbel model acceptably simulates the distributions of v_f and α.

260 The described procedure is a first attempt to statistically analyse debris flow events. The analogy
261 with other river processes, in which extreme value distributions are satisfactorily applied to describe
262 rare events such as extreme floods, is undeniable.

263

264 **Table 3.** Laboratory measurements: two statistical goodness-of-fit test results for v_f, h_f and α.

265

266 Figure 4 shows a comparison between cumulative probability distributions for v_f, h_f and α and the
267 corresponding predictive probabilistic model.

268

269 **Figure 4.** Laboratory data: comparison of cumulative probability distributions for measured and
270 theoretically predicted v_f (a), h_f (b), and α (c).

271

272 From the laboratory data it was observed that velocity, thickness and dynamic coefficient values
273 might be approximated using a GEV distribution. However, since debris flow experimental tests are
274 a scaled-down representation of the real phenomenon, presuming a GEV distribution (or any other
275 distribution) might be unjustified without a comparison with real data. The authors verified,

following the same procedure as described above, whether this hypothesis could be confirmed using the Jiangija Ravine dataset of real values.

Table 4 and Figure 5 summarize the results of the statistical analysis of the field data. Concerning v_f, the GEV distribution passed the Chi-square test but failed the AD test; however, Figure 5a clearly shows that there exists an acceptable approximation between the GEV and the cumulative distributions of the measured data, as the mean difference between the two curves is less than 10%. As for the dynamic coefficient α, this could be approximated using both the lognormal and GEV distributions. Concerning flow thickness, the Gumbel, GEV and Weibull distributions satisfied all the criteria of the GoF tests. The hypothesis was therefore confirmed: the GEV properly describes the probability distributions of thickness and velocity in flow-like phenomena.

Table 4. Field measurements: two statistical goodness-of-fit test results for v_f and h_f.

Figure 5. Field data: comparison of the cumulative probability distributions for measured and theoretically predicted v_f (a), h_f (b) and α (c).

The key point concerning the statistical treatment of debris flow events is that, while the scientific literature includes some examples of extreme value distributions satisfactorily applied to debris flow magnitude (Helsen et al. 2002; Marchi and D'Agostino 2004), no examples exist for flow characteristics due to a lack of monitoring data. However, the statistical analysis confirms that both laboratory and field parameter distributions can be approximated using a GEV distribution.

5. RBD of debris flow barriers

299 As described above, FORM requires the introduction of a performance function g(x) = 0 that
300 generally reflects the difference between resistances and the effects of actions.

301 In this research, the following equation was used:

302

303 $$g(x) = R - \rho\alpha v_f^2 h_f B \quad (5)$$

304

305 where R is barrier resistance in N, ρ is flow density in kg/m^3 (equal to 1920 kg/m^3 and 2155 kg/m^3,
306 respectively, for laboratory and field data), and B is channel width in m (equal to 0.39 m and 36 m,
307 respectively, for laboratory and field data).

308 Equation 5 represents the difference between barrier resistance and flow thrust evaluated using
309 Hungr et al.'s hydrodynamic model (1984). Dynamic impact force was calculated using the
310 momentum equation, with the impacting mass considered to be a prism travelling with uniform
311 velocity equal to mean flow velocity. Since lateral velocity variation was negligible at the flow
312 front, the front thrust results were more significant. Flow density, assumed to be constant during the
313 impact phase, was represented by a mean value for the solid and fluid components.

314 Low and Tang (1997) highlighted that correlation between variables produces a rotation of the
315 dispersion hyperellipsoid, and consequently, a variation in the probability of failure. Table 2 shows
316 that velocity and height flow and velocity and dynamic coefficient are negatively correlated, as
317 discussed in Vagnon and Segalini (2016).

318 Since the barrier is manmade and built following engineering criteria, resistance probability was
319 assumed to be normally distributed, with standard deviation equal to 3% of the mean.

320 EN1990 Annex C Table C1 gives a list of reliability index values, β, as a function of probability of
321 failure, P_f. Using those values, a RBD approach to a debris flow rigid barrier is proposed, based on

322 an analysis of both laboratory and field datasets. In particular, the design points for each variable
323 were identified and their distance from the corresponding mean was evaluated.
324
325 **Table 5.** Relationship between P_f and β.
326
327 Figure 6 depicts the Low and Tang (2007) FORM computational approach in the Microsoft Excel
328 spreadsheet platform. The spreadsheet allows the value of the reliability index, β, to be minimized,
329 starting from the main parameters that describe debris flow and their respective probabilistic
330 distributions. Required for each distribution are the mean (Para1) and standard deviation (Para2).
331 Microsoft Excel Solver automatically changes the x* column in order to find the minimum value of
332 β, by imposing two constraints: i) g(x)=0 and ii) upper limits for the GEV distributions.
333
334 **Figure 6.** Determining the reliability index β and the coordinates of the design point x* for a
335 hypothetical rigid debris flow barrier.
336
337 In Figure 6, the column x* represents the coordinates of the design point, i.e., the point where the
338 four-dimensional equivalent dispersion ellipsoid is tangential to the limit state surface. These
339 coordinates are the most probable failure combination for the debris flow parameters.
340 Listed in Table 6 as a function of the probability of failure are the combinations of design
341 parameters for the laboratory and field data. At first sight, design resistance, velocity and dynamic
342 coefficient values increase as the reliability index increases. Design thickness for laboratory data
343 seems not to be influenced by the probability of failure; rather, considering the field data, it behaves
344 similarly to the other design parameters. This behaviour is explained by smaller thickness variations

345 in the laboratory data compared to the field data.

346

347 **Table 6.** Design parameters evaluated for a reliability-based design approach as a function of
348 reliability index values proposed in EN 1990 Annex C Table C1.

349

350 As discussed in relation to the statistical analysis, the reliability method is directly correlated with
351 the partial safety factor concept introduced in EC7. In fact, the coordinates of the design point allow
352 the partial safety factors to be evaluated, as, once the probabilistic distribution of the parameters is
353 defined, the characteristic values can be back-calculated assuming the i^{th}-percentile of the
354 probability distribution. The partial safety factor is the ratio between the characteristic value and the
355 design parameter value.
356 Figure 7 shows flow barrier partial safety factor trends γ for each parameter, for laboratory data
357 (circles) and field data (squares), as a function of the probability of failure, P_f. Partial safety factors
358 were calculated considering the 50^{th}, 70^{th} and 90^{th} percentiles, indicated in black, dark grey and light
359 grey, respectively.
360 Main findings can be summarized as follow:

361 - Generally, the higher the percentile value, the lower the partial safety factor value. The
362 opposite occurs with partial safety factors for resistance, as these are reducing factors.
363 - Partial safety factors for resistance are independent from probability of failure values and are
364 the same for both laboratory and field datasets (Figure 7a). This reflects a low degree of
365 uncertainty in relation to barrier resistance evaluation.
366 - Even though the velocity and dynamic coefficient partial safety factors are different (Figures 7b
367 and 7d), their trend is the same. In fact, those two figures suggest that characteristic values for
368 v_f and α should be increased and that α should be increased more than v_f.

- Significant differences are evident for partial safety factors for thickness, as for laboratory data, they remain constant and close to unity, whereas for field data, the trend is the same as for velocity and dynamic coefficient. The most plausible explanation is the greater variability in thickness measured in the field compared to in small-scale laboratory tests.

Figure 7. Partial safety factor dependence on resistance (a), velocity (b), thickness (c) and dynamic coefficient (d) as a function of probability of failure for laboratory data (circles) and field data (squares). Three percentiles were considered for each parameter probability distribution: 50^{th} (black), 70^{th} (dark grey) and 90^{th} (light grey).

6. Summary and conclusions

Since the impact of debris flow against rigid and flexible protection structures is still not clearly understood, the design of countermeasures is problematic. First, design-related uncertainties complicate evaluation of the probability of failure, and second, further uncertainties arise in the assumptions that engineers are forced to make due to the lack of data. No clear guidelines as yet exist for the safe design of debris flow protection barriers. As pointed out elsewhere (Vagnon et al. 2016, Vagnon et al. 2017), the EC7 LSD approach based on partial safety factors is not fully applicable, since the proposed partial safety factor set does not cover the main parameters associated with debris flow phenomena. We argue that structure interaction problems can be better analysed using a RBD approach that investigates the probability of failure associated with parameter variability.

The RBD approach to designing debris flow barriers described above complements the EC7 LSD approach and highlights the associated limitations and advantages. The main limitations are data availability and the possibilities for analysing data in a statistical framework. As mentioned, the

393 lack of monitoring data for real debris flow events forces assumptions to be made regarding
394 statistical distribution.

395 In a more rigorous approach to this problem, the authors of this paper, drawing on laboratory and
396 field data, selected the probability distributions that best fit the experimental data and verified the
397 resulting probability distributions against the real dataset.

398 GEV has been demonstrated to be capable of simulating probabilistic distributions for flow height,
399 velocity and thickness. The GEV distribution is frequently used to model flood event frequencies.
400 Debris flows, we suggest, can be considered as a particular kind of riverine process and, on the
401 basis of this analogy and the results of this research underpinned by rigorous statistical calculations,
402 it should be possible to assume probabilistic extreme distributions for debris flows. However, to
403 confirm or refute this assumption, further studies would need to be done using other datasets.

404 Regarding probability distributions, an interesting finding was that both laboratory data and field
405 data follow the same statistical model, namely the GEV distribution, for all the variables. This
406 further confirms the hypothesis that small-scale laboratory tests can simulate and obtain data for
407 full-scale flow barrier design.

408 Another limitation of the RBD approach arises in the selected performance function: changing the
409 impact model causes the value of β to change and this, in turn, causes the probability of failure to
410 change. Sensitivity analyses would therefore be required in order to quantify the effect of the
411 selected performance function.

412 The RBD approach allows back-calculated partial safety factors to be applied in the LSD method
413 proposed by EC7. These partial safety factors have the advantage that they are associated with a
414 known target failure probability. However, a question remains as to the universal meaning of partial
415 safety factors for this type of geoengineering problems: the application of a set of partial safety
416 factors does not allow determination of the associated probability of failure in the Limit State

417 Design (LSD) approach, contrary to the RBD approach. Moreover, there are not enough elements
418 and accumulated experience, as in other geotechnical contexts (for instance, regarding the
419 interactions between soils and foundations), to extend the partial safety factor approach to
420 interactions between debris flows and barriers with some certainty of safety.

421 In conclusion, the RBD method provides insights into EC7 design for debris flow countermeasures
422 and is a useful design approach for protection structures based on determining an associated
423 probability of failure.

424

425 **Acknowledgement:** We gratefully acknowledge Ailish M. J. Maher for the language polishing of
426 the final version of the manuscript.

427

428

429 **References**

430 Ang HS, Tang WH (1984) Probability concepts in engineering planning and design. Decision, Risk
431 and Reliability. Vol. 2 New York: J. Wiley

432

433 Armanini A, Scotton P (1992) Experimental analysis on the dynamic impact of a debris flow on
434 structures. *In* Proceedings of the International Symposium Interpraevent, Bern, Switzerland, 107–
435 116

436

437 Baecher GB, Christian JT (2003) Reliability and statistics in geotechnical engineering. Chichester.
438 West Sussex, England: Hoboken, NJ: J. Wiley

439

440 Callisto L (2010) A factored strength approach for the limit states design of geotechnical structures.

441 Canadian Geotechnical Journal 47:1011–1023

442

443 Ditlevsen O (1981) Uncertainty modelling: with applications to multidimensional civil engineering
444 systems. New York: McGraw-Hill

445

446 Duncan JM (2000) Factors of safety and reliability in geotechnical engineering. Journal of
447 Geotechnical and Geoenvironmental Engineering 126(4):307–316

448

449 EN 1990 (2002) Eurocode - Basis of structural design. Brussels, Belgium, CEN

450

451 EN 1997-1 (2004) Eurocode 7: Geotechnical Design - Part 1: General rules. Brussels, Belgium,
452 CEN

453

454 Haldar A, Mahadevan S (1999) Probability, reliability and statistical methods in engineering design.
455 New York: J. Wiley

456

457 Harrison JP (2014) Eurocode 7 and rock engineering: current problems and future opportunities. *In*
458 Proceedings of EUROCK European Regional Symposium – Rock Engineering and Rock
459 Mechanics: Structures in and on Rock Masses, Vigo, Spain, 1531-1537.

460

461 Hasofer AM, Lind NC (1974) An exact and invariant second-moment code format. Journal of
462 Mechanical Division ASCE 100(1):111–121

463

464 Helsen MM, Koop PJM, Van Steijn H (2002) Magnitude-frequency relationship for debris flows of

the fan of the Chalance torrent, Valgaudemar (French Alps). Earth Surface Processes and Landforms 27(12):1299–1307

Hong Y, Wang JP, Li DQ et al. (2015) Statistical and probabilistic analyses of impact pressure and discharge of debris flow from 139 events during 1961 and 2000 at Jiangjia Ravine, China. Engineering Geology 187:122–134

Huang HW, Wen SC, Zhang J, et al. (2018) Reliability analysis of slope stability under seismic condition during a given exposure time. Landslides 15(11):2303-2313

Hungr O, Morgan GC, Kellerhals R (1984) Quantitative analysis of debris torrent hazard for design of remedial measures. Canadian Geotechnical Journal 21:663–667

Hubl J, Suda J, Proske D, et al. (2009) Debris flow impact estimation. *In* Proceedings of the 11th International Symposium on Water Management and Hydraulic Engineering, 37–148

Jakob M, Hungr O (2005) Debris-flow Hazards and Related Phenomena. Springer-Verlag Berlin Heidelberg

Kang ZC, Cui P, Wei FQ, He SF (2006) Data collection of observation of debris flows in Jiangjia Ravine, Dongchuan Debris Flow Observation and Research Station (1961–1984). Science Press, Beijing, China

Kang ZC, Cui P, Wei FQ, He SF (2007) Data collection of observation of debris flows in Jiangjia

489 Ravine, Dongchuan Debris Flow Observation and Research Station (1995–2000). Science Press,
490 Beijing, China
491
492 Lamas L, Perucho A, Alejano LR (2014) Some key issues regarding application of Eurocode 7 to
493 rock engineering design. *In* Proceedings of EUROCK European Regional Symposium – Rock
494 Engineering and Rock Mechanics: Structures in and on Rock Masses, Vigo, Spain, 1459-1465.
495
496 Li DQ, Xiao T, Cao ZJ, Zhou CB, Zhang LM (2016) Enhancement of random finite element
497 method in reliability analysis and risk assessment of soil slopes using Subset Simulation. Landslides
498 13(2):293–303
499
500 Low BK, Tang Wilson H (1997) Efficient reliability evaluation using spreadsheet. Journal of
501 Engineering Mechanics, ASCE 749–752
502
503 Low BK, Tang Wilson H (2004) Reliability analysis using object-oriented constrained optimization.
504 Structural Safety, 26:69–89
505
506 Low BK, Tang Wilson H (2007) Efficient spreadsheet algorithm for first-order reliability method.
507 Journal of Engineering Mechanics, ASCE 133(12):1378–1387
508
509 Low BK, Phoon KK (2015) Reliability-based design and its complementary role to Eurocode 7
510 design approach. Computer and Geotechnics 65:30–44
511
512 Madsen HO, Krenk S, Lind NC (1986) Methods of structural safety. Englewood Cliffs. NJ:

513 Prentice-Hall

514

515 Marchi L, D'Agostino V (2004) Estimation of debris-flow magnitude in the eastern Italian Alps.
516 Earth Surface Processes and Landforms 29:207–220

517

518 McGuire MP, VandenBerge DR (2017) Interpretation of shear strength uncertainty and reliability
519 analyses of slopes. Landslides 14(6):2059–2072

520

521 Melchers RE (1999) Structural reliability analysis and prediction. 2nd ed. New York: J. Wiley

522

523 Österreichischen Normungsinstituts Regeln (ONR, Austrian Standard Institute) 24800 (2009)
524 Protection works for torrent control – Terms and their definitions as well as classification. Wien,
525 Austria (in German)

526

527 Österreichischen Normungsinstituts Regeln (ONR, Austrian Standard Institute) 24802 (2011)
528 Protection works for torrent control – Design of structures. Wien, Austria (in German)

529

530 Rackwitz R, Fiessler B (1978) Structural reliability under combined random load sequences.
531 Computer& Structures 9(5):484–494

532

533 Sun HW, Lam TTM, Tsui HM (2003) Design basis for standardised modules of landslide debris-
534 resisting barriers. GEO Report 174

535

536 Vagnon F, Segalini A, Ferrero AM (2015) Studies of Flexible Barriers under Debris Flow Impact:

537 An Application to an Alpine Basin. *In* Proceedings of 1st World Multidisciplinary Earth Sciences
538 Symposium, 15: 165–172
539
540 Vagnon F and Segalini A (2016) Debris flow impact estimation on a rigid barrier. Natural Hazards
541 Earth System Sciences, 16: 1691–1697, doi:10.5194/nhess-16-1691-2016.
542
543 Vagnon F, Ferrero AM, Segalini A (2016) EC7 design approach for debris flow flexible barriers:
544 applicability and limitations. *In* Proceedings of EUROCK 2016 ISRM International Symposium -
545 Rock Mechanics and Rock Engineering: from the past to the future. Cappadocia, Turkey, 28-31
546 August 2016
547
548 Vagnon F, Ferrero AM, Segalini A, Pirulli M (2016) Experimental study for the design of flexible
549 barriers under debris flow impact. *In* Landslides and Engineered Slopes. Experience, Theory and
550 Practice 1951–1956
551
552 Vagnon F, Ferrero AM, Umili G, Segalini A (2017) A factor strength approach for the design of
553 rock fall and debris flow barriers. Geotechnical and Geological Engineering 1–13
554
555 Vagnon F, Bonetto SMR, Ferrero AM, Migliazza MR, Umili G (2020) Rock-engineering design
556 and NTC 2018: some open questions. In Geotechnical Research for Land Protection and
557 Development 519–528 DOI: 10.1007/978-3-030-21359-6_55
558
559 Zhang J, Xiong G (1997) Data collection of kinematic observation of debris flows in Jiangjia
560 Ravine, Dongchuan, Yunnan (1987–1994). Science Press, Beijing, China

Zhao L, Zuo S, Lin Y, Li L, Zhang Y (2016) Reliability back analysis of shear strength parameters of landslide with three-dimensional upper bound limit analysis theory. Landslides 13:711–724

Zhou GGD, Ng CWW (2010) Dimensional analysis of natural debris flows. Canadian Geotechnical Journal 47(7):719–729

567 **Tables**

568 **Table 1.** Principal laboratory and field dataset features.

	Dataset	Apparatus/Basin	Material	Measured Physical Quantities	Dimension of the dataset	Range of variation of parameters
Laboratory experiments	Vagnon and Segalini, 2016	Steel flume 4 m long and 0.39 m wide in which the slope varies between 30° and 35°	Saturated sand with constant liquid concentration (0.4) and mixture density (1920 kgm^{-3}). Grain size distribution varies between 0.0001 and 5 mm	Flow velocity, impact height and impact forces recorded in real time during the experiments	82 tests with different volumes and different slopes	v_f: 1.16-6.74 ms^{-1} h_f: 0.01-0.07 m α: 0.44-3.44
Field measurements	Hong et al., 2015	Jiangjia Ravine basin (near Dongchuan city, China). Area 48.6 km^2 and mainstream length 13.9 km	Bulk density ranges from 1600 to 2300 kgm^{-3} with fluid concentration ranging from 0.15 to 0.6. Solid particle dimensions vary between 0.001 and 100 mm	Channel width, flow velocity, impact height, density, duration and impact forces recorded in real time during debris flow events	139 events from 1961 to 2000	v_f: 3-20 ms^{-1} h_f: 0.1-6.4 m α: 0.06-8

569

570 **Table 2.** Main statistical parameters for the laboratory and field datasets.

Parameter	Laboratory data Value			Field data Value		
	v_f [m/s]	h_f [m]	α [-]	v_f [m/s]	h_f [m]	α [-]
Mean (μ)	3.67	0.05	1.21	10	1.6	1.36
Variance (σ^2)	1.28	0.0003	0.27	10	1.2	1.53
Standard deviation (σ)	1.13	0.02	0.52	3	1.1	1.24
Coefficient of variation (CV)	0.31	0.35	0.43	0.33	0.69	0.91
Asimmetry coefficient (γ)	0.69	-0.45	1.62	0.22	1.12	2.71
Maximum	6.74	0.07	3.44	20	6.4	8.01
Minimum	1.16	0.01	0.44	3	0.1	0.06
Coefficient of correlation v-h		-0.6			-0.6	
Coefficient of correlation v-α		-0.5			-0.5	
Coefficient of correlation h-α		-			-	
Number of experimental tests		82			139	
Number of classes (defined using Equation 3)		12			14	

571

572 **Table 3.** Laboratory measurements: two statistical goodness-of-fit test results for v_f, h_f and α.

Variable	Results		Probabilistic model						
			Normal	**Lognormal**	**Exponential**	**Gumbel**	**GEV**	**Gamma**	**Weibull**
v_f	Chi-square test	χ^2	17.51	80.44	153.32	9.90	15.34	20.63	19.95
	Critical value	χ^2_{lim}	16.92	16.92	18.31	16.92	15.51	16.92	16.92
	Suitability		NO	NO	NO	YES	YES	NO	NO
	AD test	A^2				0.196	0.458		
	Critical value	A^2_{lim}				0.461	0.461		
	Suitability					YES	YES		
h_f	Chi-square test	χ^2	19.27	399.46	126.39	28.05	8.44	18.98	13.80
	Critical value	χ^2_{lim}	16.92	16.92	18.31	16.92	15.51	16.92	16.92
	Suitability		NO	NO	NO	NO	YES	NO	YES
	AD test	A^2					0.279		0.917
	Critical value	A^2_{lim}					0.461		0.461
	Suitability						YES		NO
α	Chi-square test	χ^2	16.34	146.29	97.41	14.88	13.41	22.59	64.93
	Critical value	χ^2_{lim}	16.92	16.92	18.31	16.92	15.51	16.92	16.92
	Suitability		YES	NO	NO	YES	YES	NO	NO
	AD test	A^2	2.65			0.283	0.440		
	Critical value	A^2_{lim}	0.46			0.461	0.461		
	Suitability		NO			YES	YES		

573

574 **Table 4.** Field measurements: two statistical goodness-of-fit test results for v_f and h_f.

Variable	Results		Probabilistic model						
			Normal	**Lognormal**	**Exponential**	**Gumbel**	**GEV**	**Gamma**	**Weibull**
$\mathbf{v_f}$	Chi-square test	χ^2	25.64	42.44	196.54	29.37	22.73	24.81	26.05
	Critical value	χ^2_{lim}	24.72	24.72	26.22	24.72	23.21	24.72	24.72
	Suitability		NO	NO	NO	NO	YES	NO	NO
	AD test	A^2					0.93		
	Critical value	A^2_{lim}					0.461		
	Suitability						NO		
$\mathbf{h_f}$	Chi-square test	χ^2	26.88	39.53	33.93	8.21	8.21	12.78	8.63
	Critical value	χ^2_{lim}	19.68	19.68	21.03	19.68	18.31	18.68	19.68
	Suitability		NO	NO	NO	YES	YES	YES	YES
	AD test	A^2				0.230	0.447	0.471	0.119
	Critical value	A^2_{lim}				0.461	0.461	0.461	0.461
	Suitability					YES	YES	NO	YES
$\boldsymbol{\alpha}$	Chi-square test	χ^2	96.99	18.79	59.47	67.33	12.99	45.13	44.30
	Critical value	χ^2_{lim}	19.68	19.68	21.03	19.68	18.31	18.68	19.68
	Suitability		NO	YES	NO	NO	YES	NO	NO
	AD test	A^2		-13.91			-7.67		
	Critical value	A^2_{lim}		0.461			0.461		
	Suitability			YES			YES		

575

576 **Table 5.** Relationship between P_f and β.

P_f	1.00E-01	1.00E-02	1.00E-03	1.00E-04	1.00E-05	1.00E-06	1.00E-07
β	1.28	2.32	3.09	3.72	4.27	4.75	5.2

577

578 **Table 6.** Design parameters evaluated after RBD approach as a function of reliability index values
579 suggested by Annex C of EN 1990.

β [-]	P_f [-]	Laboratory data				Field data			
		R* [N]	v_f* [m/s]	α* [-]	h_f* [m]	R* [N]	v_f* [m/s]	α* [-]	h_f* [m]
1.28	1E-01	811.98	4.12	1.27	0.05	5.70E+07	12.17	2.22	2.24
2.32	1E-02	1219.21	4.72	1.46	0.05	1.60E+08	14.19	3.29	3.12
3.09	1E-03	1639.49	5.22	1.61	0.05	3.18E+08	15.57	4.28	3.96
3.72	1E-04	2089.45	5.31	1.98	0.05	5.35E+08	16.57	5.24	4.79
4.27	1E-05	2589.75	5.45	2.39	0.05	8.15E+08	17.35	6.20	5.63
4.75	1E-06	3129.86	5.52	2.77	0.05	1.16E+09	17.96	7.15	6.45
5.2	1E-07	3719.91	5.57	3.23	0.05	1.57E+09	18.47	8.12	7.30

580

581 **Figures**

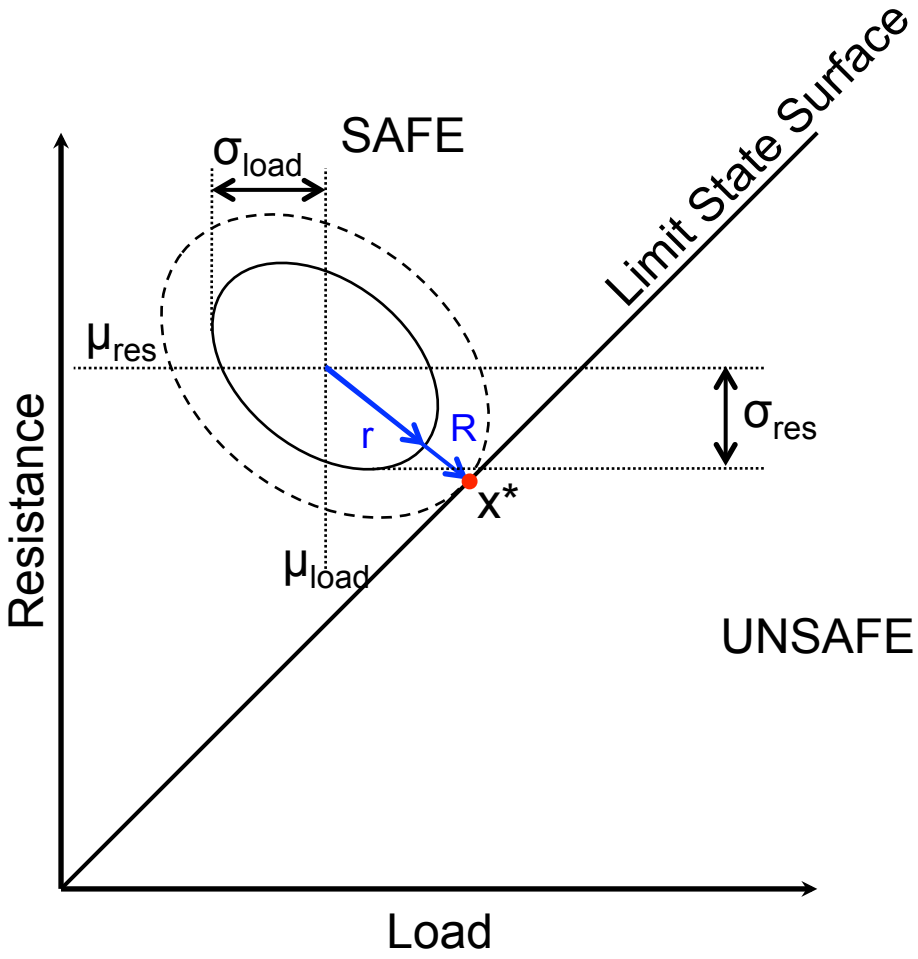

582

583 **Figure 1.** Illustration of the reliability index in a plane with two negatively correlated random
584 variables.

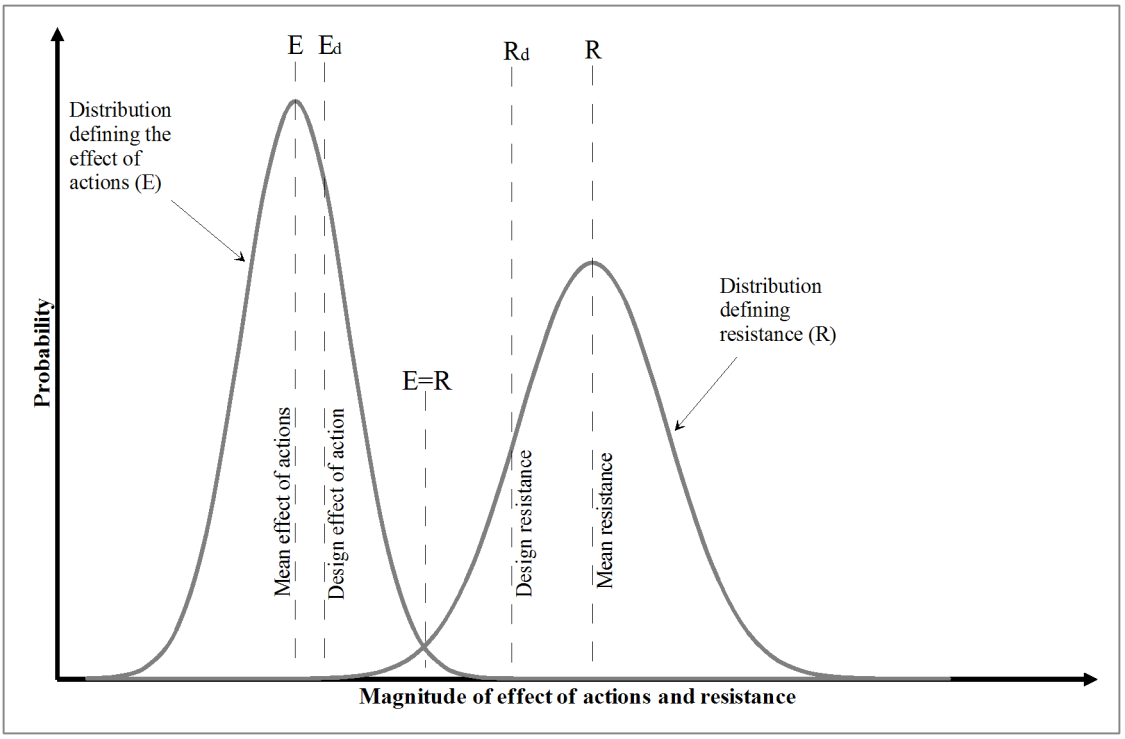

585

586 **Figure 2.** EC7 limit state design: probabilities of actions and material resistance.

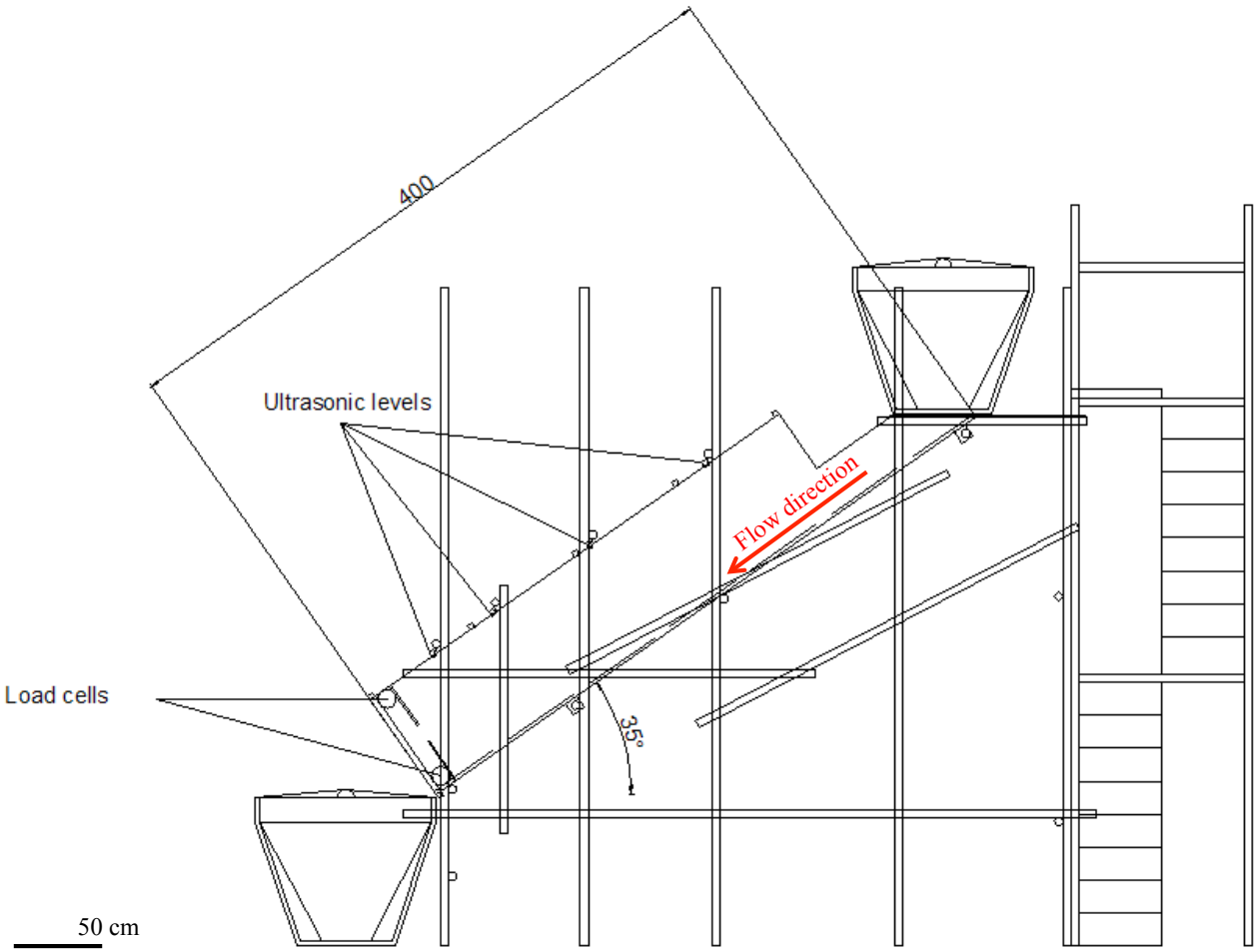

Figure 3. Flume setup and location of measurement devices.

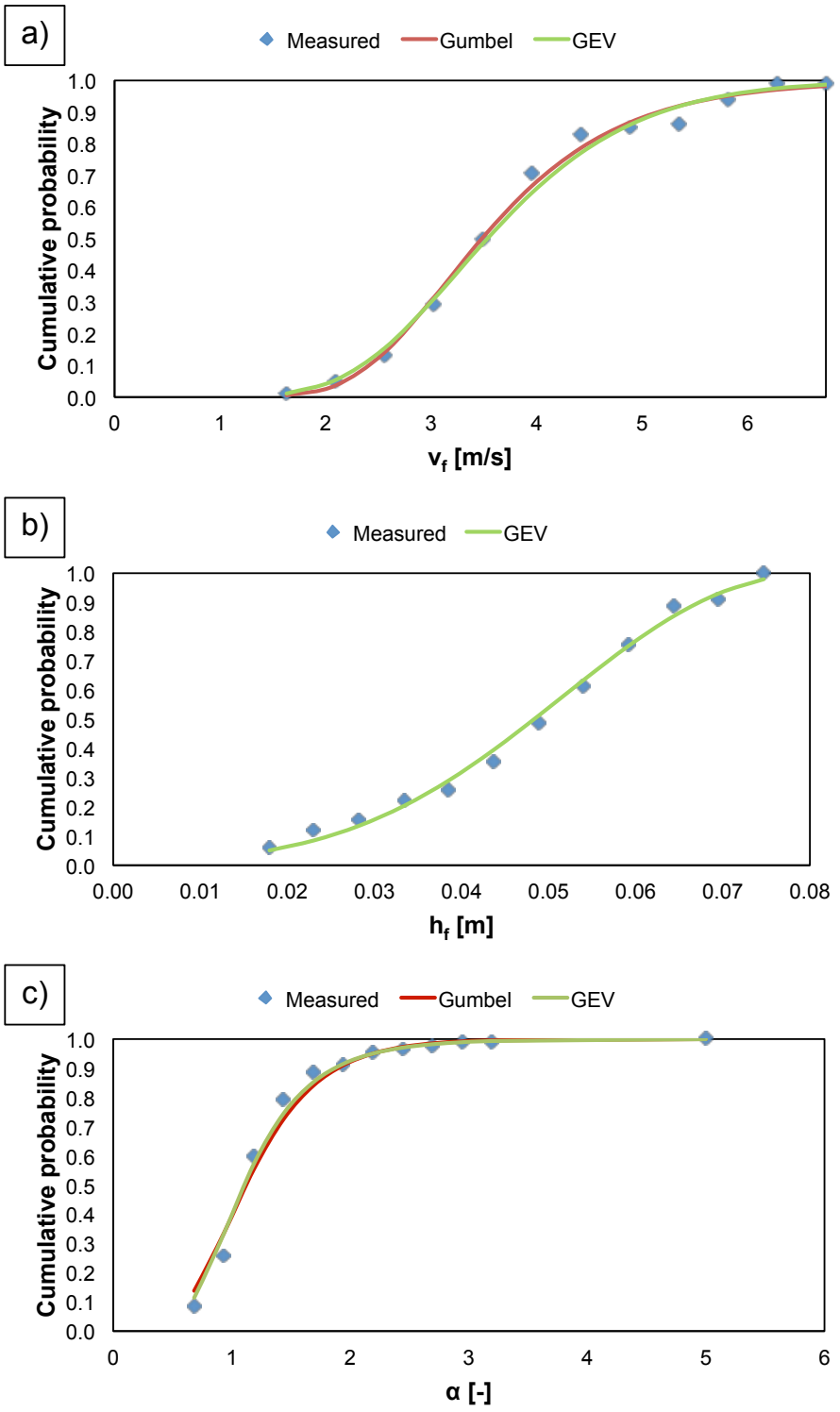

589

590 **Figure 4.** Laboratory data: comparison of cumulative probability distributions for measured and
591 theoretically predicted v_f (a), h_f (b), and α (c).

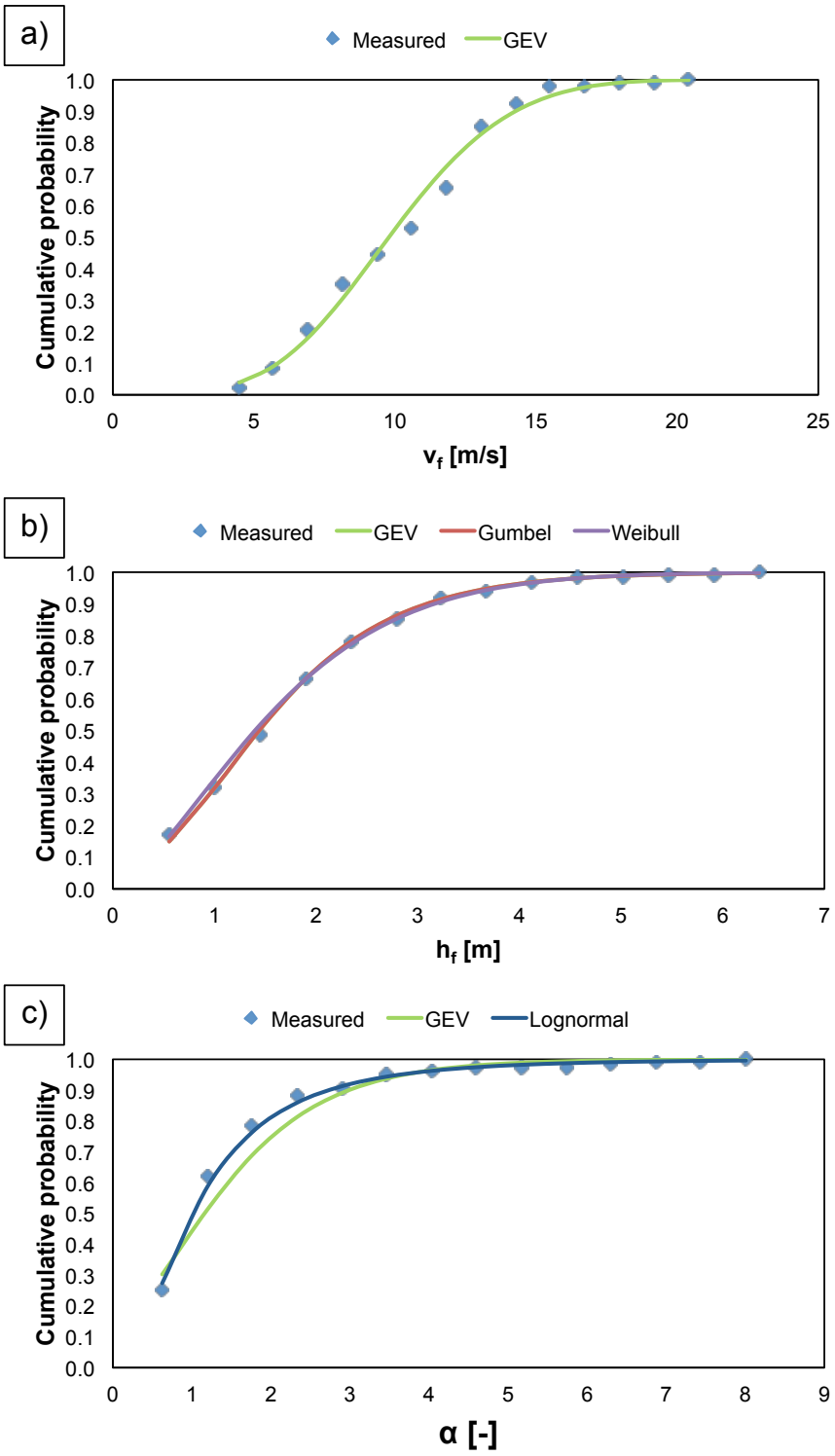

592

593 **Figure 5.** Field data: comparison of the cumulative probability distributions for measured and

594 theoretically predicted v_f (a), h_f (b) and α (c).

Distribution		Para1	Para2	x*	μ^N	σ^N
Normal	R	1570000000	4.71E+07	1.57E+09	1.57E+09	4.71E+07
GEV	vf	10	3	18.47	10.87	3.01
GEV	alfa	1.36	1.24	8.12	-3.12	3.43
GEV	hf	1.6	1.1	7.30	-2.03	2.97

Correlation matrix [R]				n
1	0	0	0	-2E-14
0	1	-0.5	-0.6	3E+00
0	-0.5	1	0	3E+00
0	-0.6	0	1	3E+00

g(x)	β
0	5.20

Probability of failure
0.00001%

595

596 **Figure 6.** Determining the reliability index β and the coordinates of the design point x* for a
597 hypothetical rigid debris flow barrier.

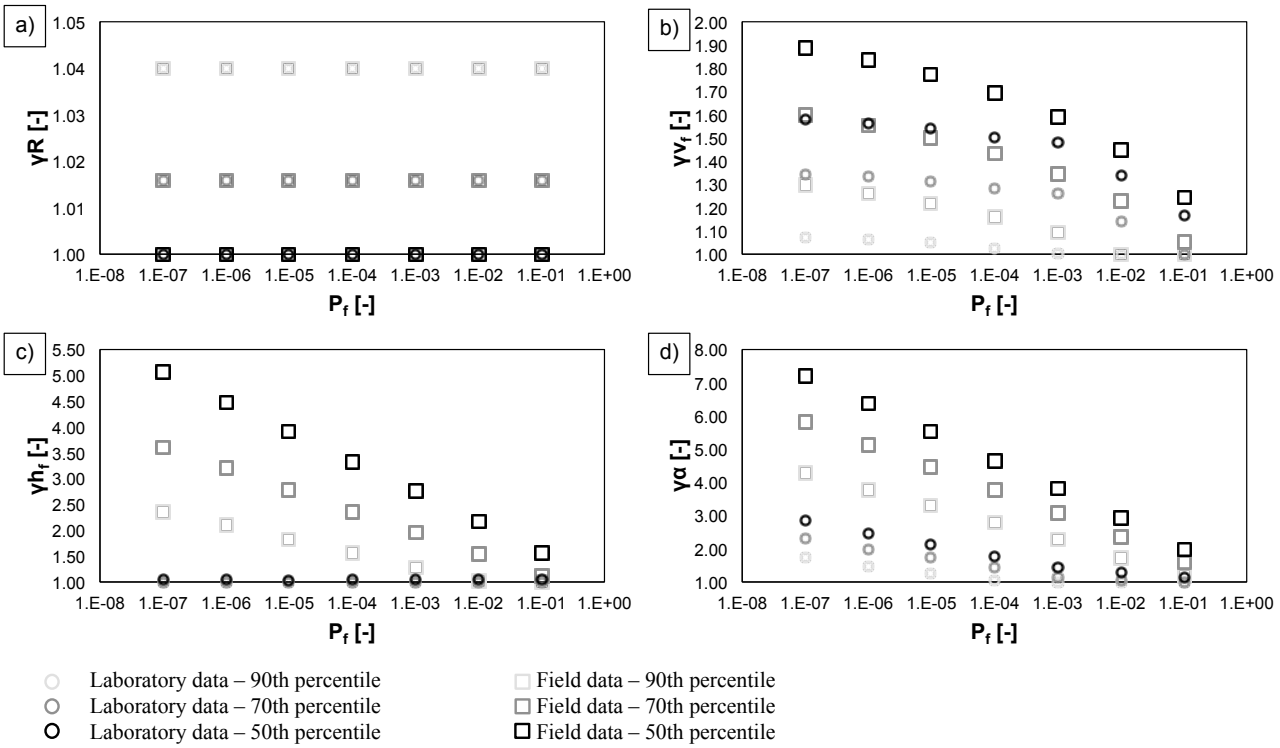

598

599 **Figure 7.** Partial safety factor dependence on resistance (a), velocity (b), thickness (c) and dynamic
600 coefficient (d) as a function of probability of failure for laboratory data (circles) and field data
601 (squares). Three percentiles were considered for each parameter probability distribution: 50th
602 (black), 70th (dark grey) and 90th (light grey).